Electronic Supplementary Material (ESI) for Journal of Materials Chemistry B.

Supplementary Information

Polyelectrolyte Complexation via Viscoelastic Phase Separation Results in Tough and Self-Recovering Porous Hydrogels

Kohei MURAKAWA,[a] Daniel R. KING,[bc] Taolin SUN,[bcd] Honglei GUO,[b] Takayuki KUROKAWA[bc] and Jian Ping GONG*[bce]

---

[a] *Graduate School of Life Science, Hokkaido University, Sapporo, 001-0021, Japan.*

[b] *Faculty of Advanced Life Science Hokkaido University, Sapporo, 001-0021, Japan*

[c] *Global Station for Soft Matter, Global Institution for Collaborative Research and Education (GI-CoRE), Hokkaido University, Sapporo, 001-0021, Japan*

[d] *South China Advanced Institute for Soft Matter Science and Technology, South China University of Technology, Guangzhou, 381st Wushan Road, Tianhe District, 510640, China*

[e] *Institute for Chemical Reaction Design and Discovery (WPI-ICReDD), Hokkaido University, Sapporo, 001-0021, Japan*

E-mail: gong@sci.hokudai.ac.jp (J. P. Gong)

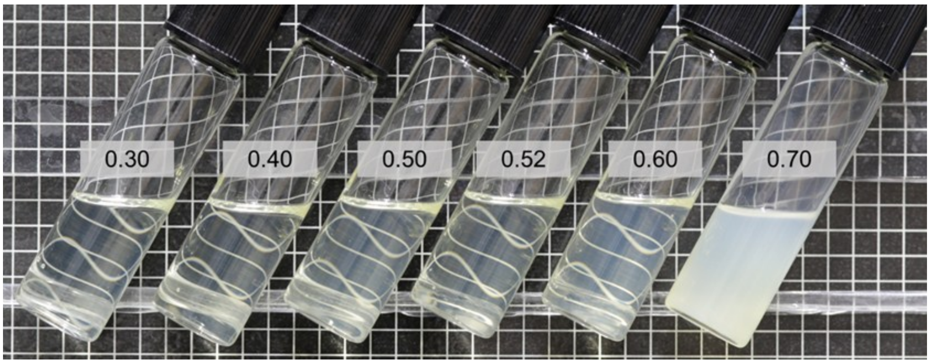

Figure S1. Appearance of polymer solutions with different anion fraction, *f*, at 25 °C where the total polymer concentration, C_p, is 1.0 M in 3.7 M NaCl. The numbers in the image represent the *f* value.

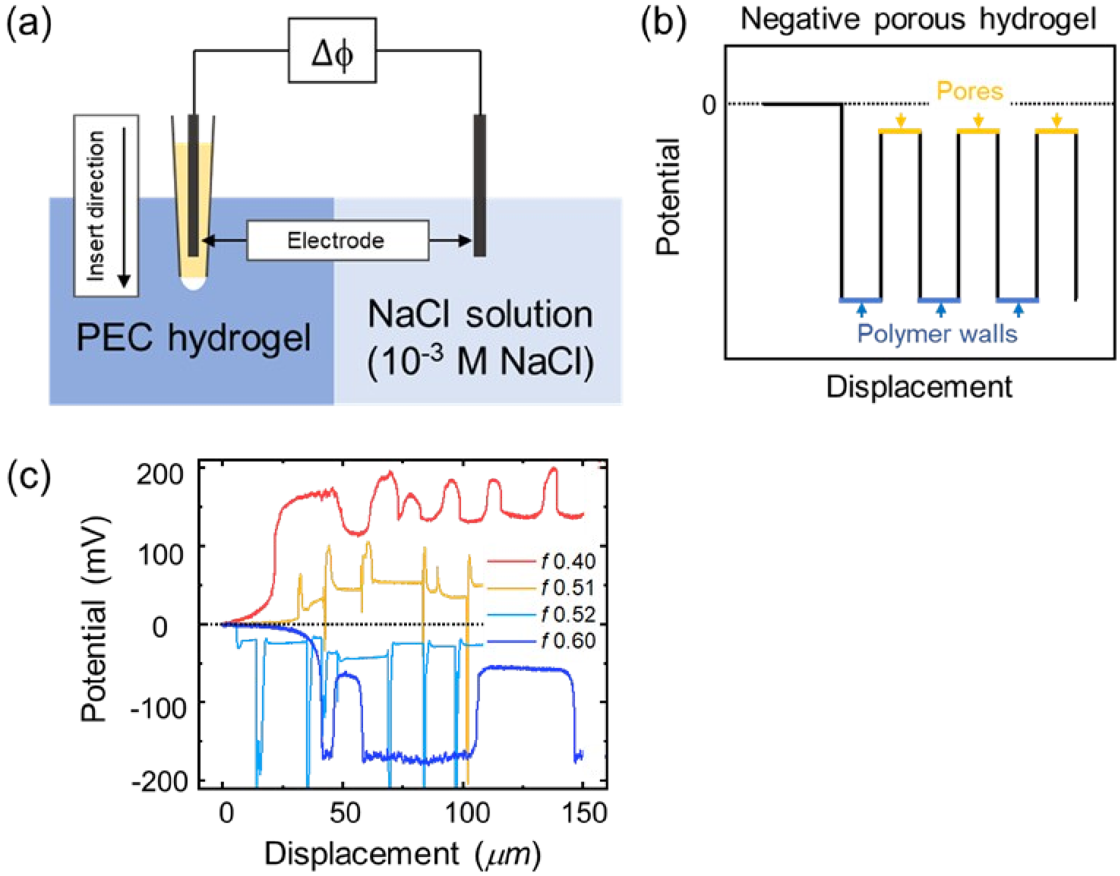

Figure S2. Donan potential of PEC hydrogels (*f*-1.0-0.3) prepared with different anion fraction, *f*. (a) Schematic illustration of Donnan potential measurements. The PEC hydrogels were immersed in 10^{-3} M NaCl solution for over 3 days before the measurement. The insertion speed of the working electrode into the hydrogels was controlled at 197.5 nm s^{-1}. The electrode was connected to an oscilloscope with a high-impedance intracellular preamplifier to measure the potential difference between the two electrodes. (b) Schematic illustration of a potential versus displacement curve of negatively charged porous hydrogels. The peaks of the curve represent the polymer walls and drops of the absolute value of the potential correspond to the interior of the pores because polymer walls have a high charge density. (c) Potential versus displacement curves of PEC hydrogels prepared with different anion fraction, *f*. The shift from positive to negative happens between $f = 0.51$ and 0.52. The peaks of the curve represent the polymer walls and drops of the absolute value of the potential correspond to the interior of the pores.

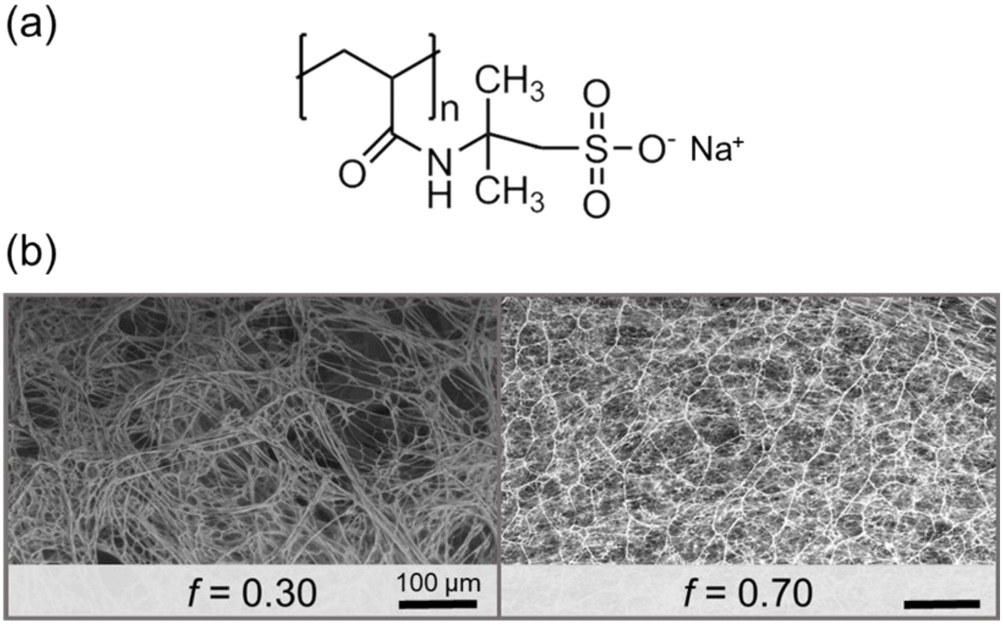

Figure S3. Morphology of PEC hydrogels (*f*-1.0-0.3) prepared with different anion fraction, *f* from poly (2-acrylamido-2-methyl-1-propanesulfonic acid sodium salt), PNaAMPS, and PDADMAC. (a) The chemical structure of PNaAMPS. The polymer is synthesized from 2-acrylamido-2-methyl-1-propanesulfonic acid sodium salt, NaAMPS. The monomer concentration is 0.5 M. α-ketoglutaric acid is used as a photo initiator with a concentration of 0.6 mol% relative to the monomer. Polymerization proceeds via UV exposure for 8 hours under an argon atmosphere. The polymer was purified by precipitation with acetone as a poor solvent to remove unreacted monomers. NaAMPS was purchased from Towa Synthetic Industrial Co. and α-ketoglutaric acid was purchased from FUJIFILM Wako Pure Chemical Industries, Ltd. From the GPC results, the average M_w is estimated to be about 1,200,000. (b) SEM micrographs of the surfaces of the PEC samples prepared with different anion fraction, *f*, 0.3 and 0.7. The micrographs were taken in the wet state under a low vacuum pressure mode.

Supplementary Section 4. Polymer Concentration Effect

Polymer concentration is one of the critical factors in determining the properties of the PEC hydrogels, because the entanglement density strongly depends on the concentration. Figure S4(a) contains images of the polymer solutions prepared with different polymer concentrations in 3.7 M NaCl, where anion fraction, f, is 0.52. At low concentration ($C_p \leqq 0.4$ M), the precipitation or coacervation occurs easily because the state is more stable thermodynamically. When C_p increases ($C_p \geqq 0.6$ M), the solution becomes homogenous, either transparent or turbid. Here, we prepared PEC hydrogels with sufficiently high C_p ($C_p \geqq 0.8$ M) because the solution is uniform and transparent. NaCl concentration for the first dialysis, C_s, is 0.3 M. Hydrogels with C_p lower than 0.8 M swell and do not form a homogenous structure.

Figure S4(b) presents the effect of C_p on the swelling volume ratio, Q_v, and water content, w. The hydrogels shrink ($Q_v < 1$) with $C_p \leqq 1.0$ M, and swell ($Q_v > 1$) with $C_p \geqq 1.2$ M. One interesting point is that even when the charge balance is almost neutral, the samples swell with high polymer concentration.

Figure S4(c) shows SEM images of the surfaces. The porous structure that forms at $C_p = 0.8$ is different from the structure formed at $C_p = 1.0$ and 1.2, and the surfaces of samples with high polymer concentration ($C_p \geqq 1.4$ M) do not have pores on the surface, while they have a porous interior. The surfaces without porous structures might cause the swelling behavior described above. The counter-ions dissociate from the surface, resulting in complexation occurring at the surface. The surface then works as a semipermeable membrane, where counter-ions cannot easily diffuse out in comparison to water molecules that can diffuse in. From these results, we see that the porous structure on the surface can be affected by polymer concentration, but the mechanism is not straightforward.

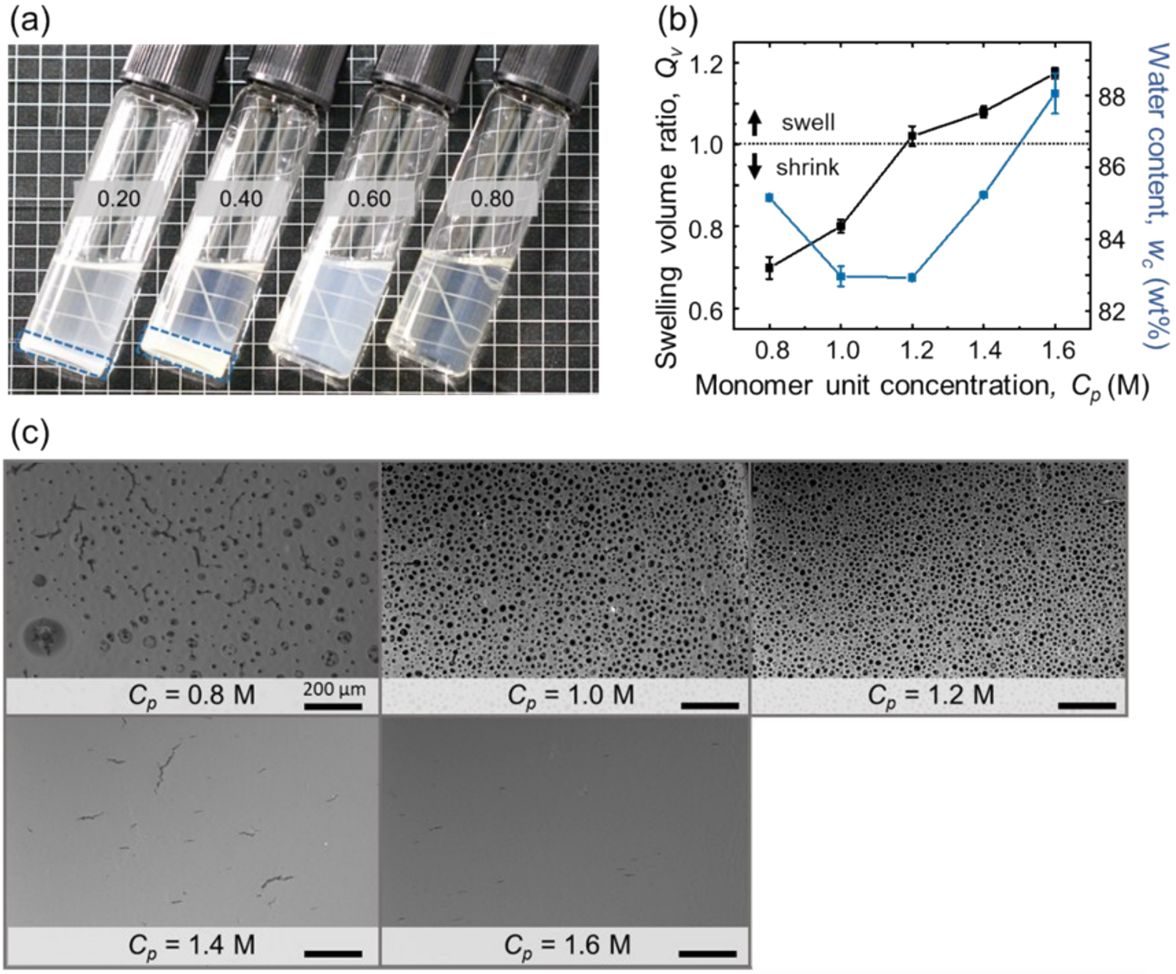

Figure S4. Appearance of the polymer solution in 3.7 M NaCl, where *f* is 0.52, and morphology of the corresponding PEC hydrogels (0.52-C_p-0.3) prepared with different monomer unit concentration, C_p. (a) Appearance of polymer solutions prepared with different monomer unit concentrations, C_p. The areas surrounded by dotted lines show the complexes and coacervate by phase separation with $C_p = 0.2$ M and 0.4 M, respectively. (b) The swelling volume ratio, Q_v, and water content, w_c, on the monomer unit concentration, C_p. (c) SEM micrographs of the surfaces of the PEC samples prepared with different monomer unit concentration, C_p. The micrographs were taken in the wet state under a low vacuum pressure mode.

Supplementary Section 5. Salt concentration effect in the first dialysis step

Salt concentration in the solution used for the first dialysis step, C_s, should affect the relaxation of the PEC hydrogels. The dialysis environment with high salt concentration would relax the ionic associations and with low salt concentration fix the complexes quickly. The mold used during the desalting process for the samples (0.52-1.0-C_s) was firstly immersed in NaCl aqueous solutions ranging from 0 ~ 3.0 M for 2 days. After this, the mold was immersed in deionized water for 7 days. Figure S5(a) presents the effect of C_s on the swelling volume ratio, Q_v, and water content, w_c, and Figure S5(b) contains SEM images of the surfaces. The hydrogels shrink more with high salt concentration, although a large difference cannot be observed on the surface. This might be because the high salt concentration dialysis environment causes the desalting process to occur more slowly and relaxes the ionic associations to a more stable state, without a porous structure.

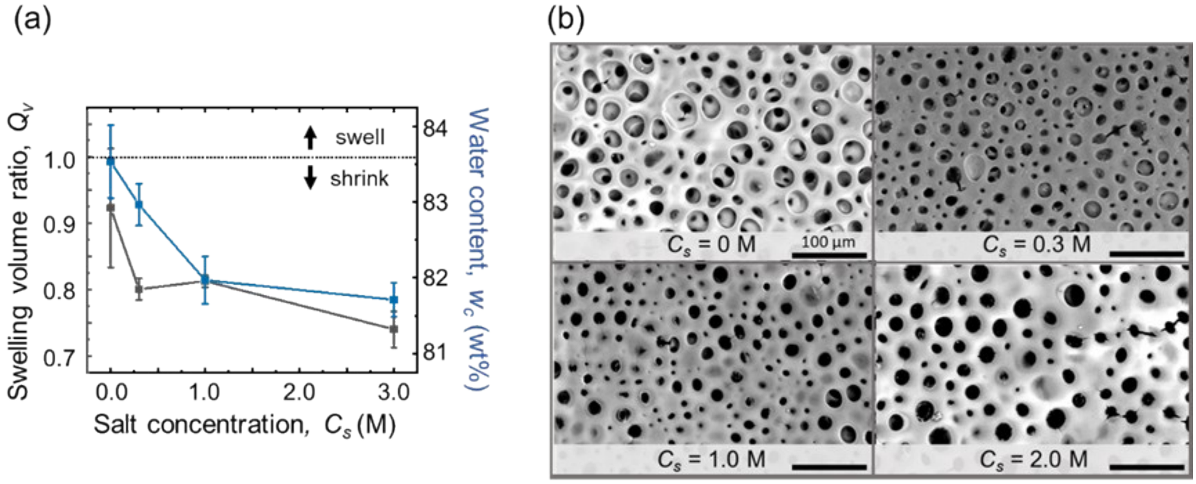

Figure S5. Morphology of PEC hydrogels (0.52-1.0-C_s) prepared with different salt concentrations in the first dialysis step, C_s. (a) The swelling volume ratio, Q_v, and water content, w_c, as a function of C_s. (b) SEM micrographs of the surfaces of the PEC samples prepared with different C_s. The micrographs were taken in the wet state under a low vacuum pressure mode.

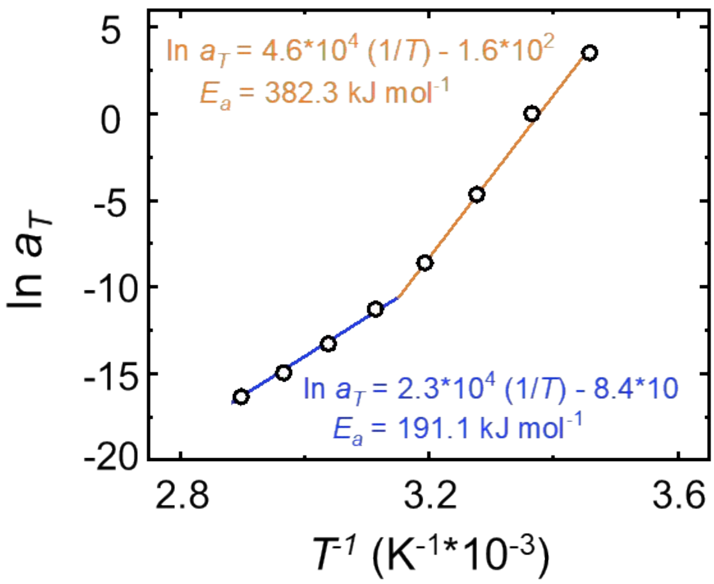

Figure S6. Arrhenius plot of the shift factors, a_T versus the inverse temperature. The apparent activation energy value, E_a, was estimated from the slope of the line using the Arrhenius equation $a_T = Ae^{E_a/RT}$, where a_T represents the shift factor from time-temperature superposition shifts with 24 ℃ as the reference temperature, where R is the ideal gas constant and A is a constant value.

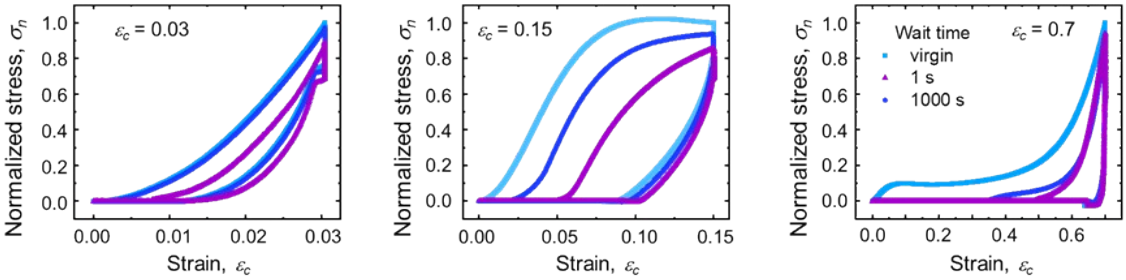

Figure S7. Normalized stress-strain curves from cyclic compression tests at ε_c = 0.03, 0.15, 0.70 with $\dot{\varepsilon}_c$ = 8.3*10^{-3} s^{-1}. Only wait times of 1 and 1000 s are shown. Normalized stress, σ_n, is calculated from the compression stress divided by the compression stress of the first cycle at the corresponding ε_c.

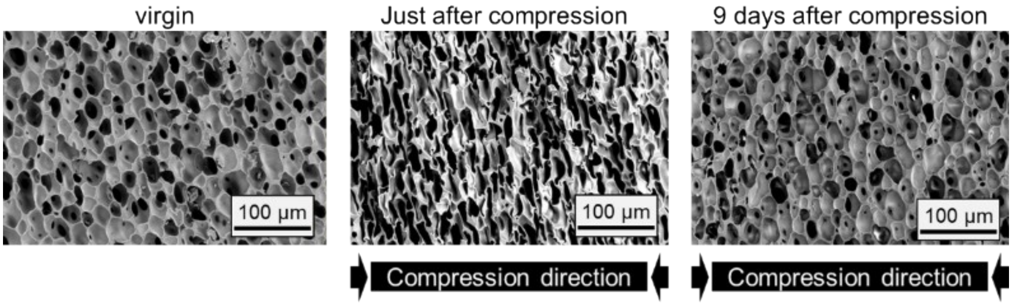

Figure S8. SEM micrographs of the cross sections of the compressed samples with different wait times after compression at $\varepsilon_c = 0.70$ with $\dot{\varepsilon}_c = 8.3*10^{-3}$ s^{-1}. The micrographs were taken under a low vacuum pressure mode.